Identifying low-frequency earthquakes in central Cascadia using cross-station correlation

Amanda M. Thomas [a,b,*], Michael G. Bostock [c]

[a] Department of Geophysics, Stanford University, Stanford, CA, USA
[b] Department of Geological Sciences, University of Oregon, Eugene, OR, USA
[c] Department of Earth, Ocean and Atmospheric Sciences, The University of British Columbia, Vancouver, BC, Canada

ARTICLE INFO

ABSTRACT

We use stations in the Willamette valley and Oregon coast ranges to identify low-frequency earthquakes that occurred during the August–September 2009 episodic tremor and slip event. While autocorrelation techniques are often successful at identifying LFE templates, in central Cascadia, this technique systematically fails due to the lack of densely spaced, high-quality stations. Instead, we use cross-station methods that have been successful at identifying LFEs in northern Cascadia to register initial candidate templates, network cross-correlation to register additional LFE detections, and stacking to refine the identified templates. Using this procedure, we detect nearly 16 thousand events comprising a total of 18 LFE families located in central Oregon between 30 and 40 km depth either at or near the plate boundary. The time history of detections between families is consistent with the slip front in the 2009 SSE migrating from north to south at a velocity of 5 km/day. The templates we identify have more complicated waveforms than those previously identified in northern Cascadia. These differences in waveform character likely a consequence of the small number of contributing stations.

© 2015 Elsevier B.V. All rights reserved.

1. Introduction

While many slow earthquakes are aseismic and can only be detected using geodetic techniques, some slow earthquakes do have a seismic manifestation. These long-duration, small-amplitude seismic signals, dubbed non-volcanic tremor (NVT) lack impulsive phase arrivals associated with regular earthquakes and are depleted in high-frequency content relative to conventional earthquakes of the same size (Ide et al., 2007; Obara, 2002). Low-frequency earthquakes (LFEs) are short-duration seismic signals also associated with slow slip that more closely resemble conventional earthquakes. Shelly et al. (2007) first demonstrated that the NVT signal can be explained as a superposition of many LFEs.

LFEs have now been observed along major strike-slip plate boundaries such as the San Andreas fault in California (Shelly and Hardebeck, 2010) and the Alpine fault in New Zealand (Chamberlain et al., 2014), in thrust faults (Tang et al., 2010), and in subduction zones around the world (Bostock et al., 2012; Brown et al., 2009; Frank et al., 2013; Plourde et al., 2015; Royer and Bostock, 2014; Rubin and Armbruster, 2013; Shelly et al., 2006). In Cascadia, high-quality LFE catalogs extend from central Vancouver Island south to approximately the Washington-Oregon border (Royer and Bostock, 2014). However, NVT regularly occurs much further south, in Oregon and Northern California (Boyarko and Brudzinski, 2010; Wech and Creager, 2008).

In this study, we attempt to find LFEs in central Cascadia from the 2009 slow slip event (SSE). We chose this episode because both the NVT data and spatiotemporal slip inversions derived from geodetic data show that slip propagates into central Oregon and ceases just south of 44° latitude (Bartlow et al., 2011; Wech and Creager, 2008). Assembling a high-quality LFE catalog in this region is challenging for two reasons. First, the low amplitude nature of LFEs requires stations that are densely spaced, have high SNR, and are close to the LFE source region, while station spacing in the central Oregon coast ranges is generally sparse. Second, LFEs in this area tend to occur in rapid bursts that form tectonic tremor and identification of individual LFEs is difficult. The challenging conditions are not unique to Oregon, hence finding approaches to identify and catalog LFEs under non-ideal conditions is important. Additionally, along strike variations in plate interface, properties such as coupling, seismicity, and resistivity provide an opportunity to identify which physical factors affect the distribution and waveform character of LFEs (Burgette et al., 2009; Tréhu et al., 2008; Wannamaker et al., 2014).

2. Methods

We use a combination of stations from the Global Seismic Network, the Plate Boundary Observatory, the Central Oregon Locked Zone Array (COLZA) (Williams et al., 2011), the Flexarray Along Cascadia

* Corresponding author at: Department of Geological Sciences, University of Oregon, Eugene, Oregon, USA.
  E-mail address: amthomas@uoregon.edu (A.M. Thomas).

Experiment, and the Pacific Northwest Seismic Network (PNSN) (Fig. 1). Data from all high gain stations operating in west central Oregon were downloaded from the IRIS DMC. Data were demeaned, detrended, band-pass filtered between 1 and 10 Hz, resampled to 40 sps, and stored in 24 h data files. In our first attempt to identify LFEs, we employed standard network autocorrelation techniques that have been successful in other subduction zone localities (Brown et al., 2009). Network autocorrelation typically involves autocorrelating records on each station channel for a subset of quality stations over a specified time period, in our case 1 h. The resulting time series are then stacked to create a network autocorrelation function. When the network autocorrelation function exceeds a given threshold (typically eight times the median absolute deviation, 8*MAD), the corresponding window pairs are considered a detection. Detections are then culled to eliminate duplicates and retain only high-quality detections (Royer and Bostock, 2014).

We applied network autocorrelation to 3 days of continuous data (09/03–09/05) during the 2009 SSE. Despite the prevalence of identifiable tremor on most stations during the time periods selected, the network autocorrelation method failed to identify a single LFE template. This is likely due to the station spacing (approximately 30 km on average), which is too sparse for there to be simultaneous, coherent LFE signal above the noise levels on more than one or two stations.

We also note that we experimented with window durations and adjusted the timing of windows to capture move out across the network for sources in the tremor catalog of Wech and Creager (2008), as other methods developed to identify LFEs have employed similar corrections (Frank and Shapiro, 2014). However, these improvements did not result in successful LFE identification.

We then adopted a cross-station approach to identify LFEs which relies on the similarity of contemporaneous waveforms between stations (Rubin and Armbruster, 2013; Savard and Bostock, 2014). We applied the method of Savard and Bostock (2014) to stations ALP0, ALS0, and BWO0 to detect candidate templates due to their generally high signal-to-noise ratios and proximity to the 2009 SSE. Once candidate templates are identified, we use network cross-correlation on 3 days of data to register additional detections defined as times when the network cross-correlation exceeds eight times the median absolute deviation. Detections are then stacked to create a new template with better SNR (Gibbons and Ringdal, 2006). To further improve the SNR, we use a technique known as phase-weighted stacking on the intermediate iterations, which incorporates phase information by upweighting sections of the stack that are coherent in phase and downweighting those that are not (Schimmel and Paulssen, 1997; Thurber et al., 2014). In order to refine the templates, we iteratively apply cross-correlation and stacking until no additional detections are registered
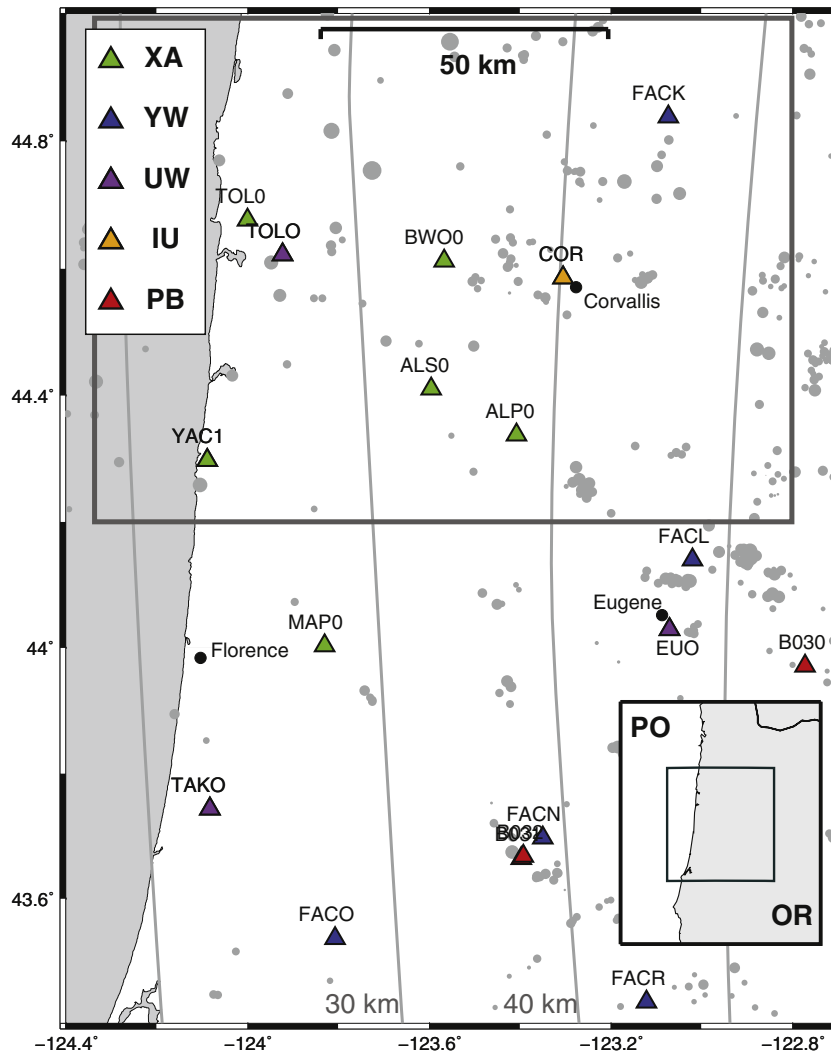
Fig. 1. Distribution of stations used to search for LFEs in Central Cascadia. Triangles mark station locations and gray contours mark the depth to the plate interface using the McCrory et al. (2004) model. Circles are locations of regional earthquakes occurring since 2000. The gray box outlines the region shown in Fig. 3. Insets are a regional location map labeling the Pacific Ocean (PO) and state of Oregon (OR) and a legend of network codes of the stations we used to detect LFEs. XA-COLZA, YW-Flexarray Along Cascadia Experiment, UW-PNSN, IU-Global Seismographic Network, PB-Plate Boundary Observatory. (For interpretation of the references to color in this figure legend, the reader is referred to the web version of this article.)

(generally 10–15 iterations). If additional stations begin to show coherent energy, those stations are included in network correlation upon subsequent iterations. We require a minimum of 100 detections in the 3-day window to stack an LFE template. LFE templates that make the cut are cross-correlated through 46 days of continuous data from August 3 through September 17, 2009. We eliminate duplicate families by ensuring that no family shares more than 10% of detection times, defined as a difference between detection times of <5s, with any other family. Finally, the remaining LFE families are located using HYPOINVERSE (Klein, 2002) with two different velocity models. The first is the O0 model, a regional velocity model employed by the PNSN for earthquake location, and the second is a local 1D model employed by Williams et al. (2011) derived from the 2D model of Gerdom et al. (2000).
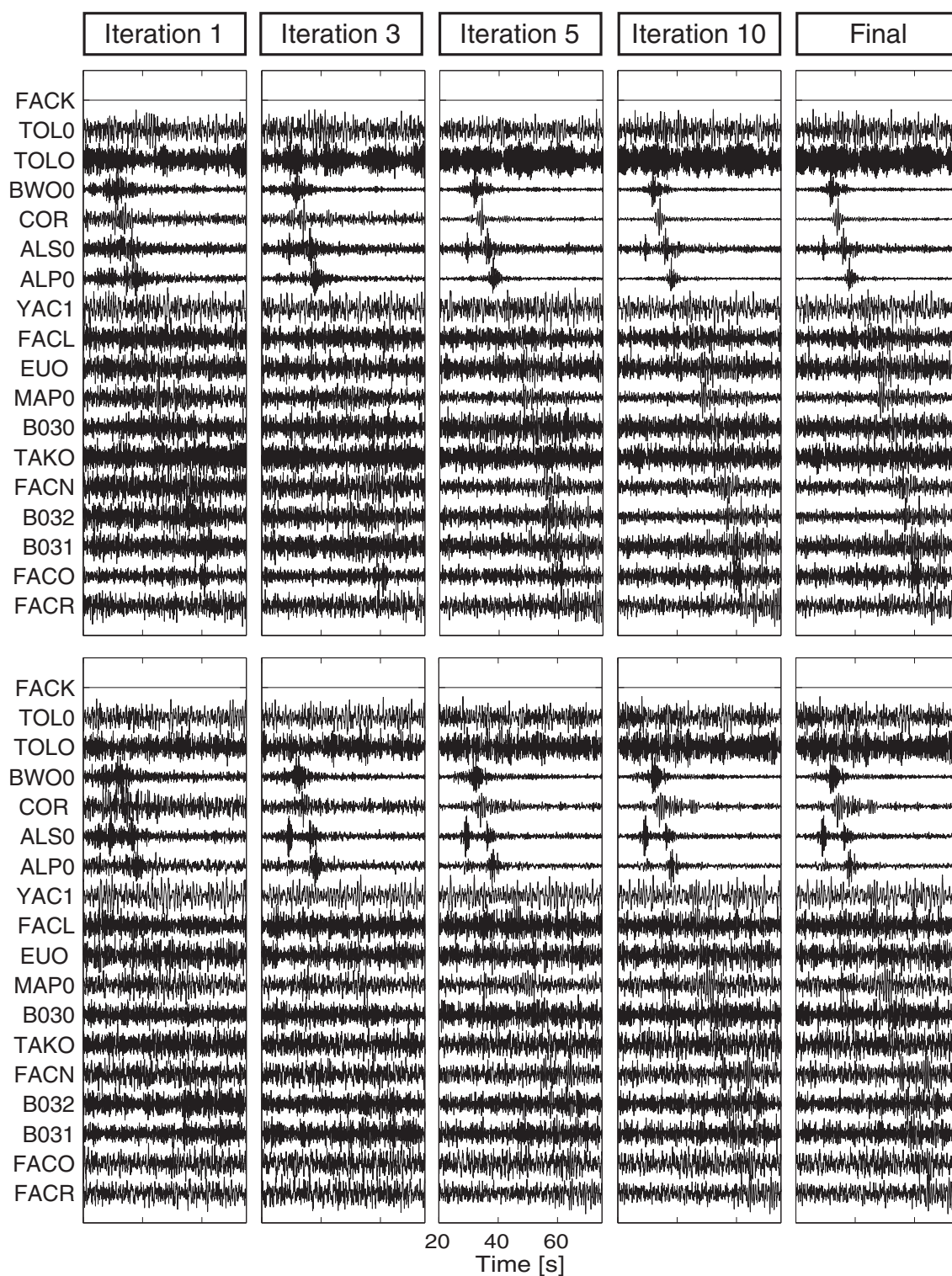
Fig. 2. Horizontal (top row) and vertical (bottom row) component seismograms at all stations used in this study showing an example of the evolution of an LFE template throughout the iterative network cross-correlation procedure described in Section 2.

3. Results

Fig. 2 shows one of the best examples of LFEs emerging from the iterative network cross-correlation procedure described above. Initially, the stack does not include station COR, but after the first iteration, a coherent signal emerges at COR and is incorporated into the network correlation function. Additionally, in later iterations, move out becomes visible on many of the stations further south, such as MAP0, B031, and B032, which were not employed in the scanning template supporting the veracity of the registered detections.

In total, the combined cross-station and iterative network cross-correlation procedure described above resulted in a total of 18 families and over 15,000 individual LFE detections. Of these 18, we were unable to locate five families because the templates were not of sufficient quality to accurately pick arrivals. The LFE locations are shown in Fig. 3 and generally cluster near and within a group of densely spaced high-quality stations deployed near Corvallis as part of COLZA (Williams et al., 2011). Due to the paucity of visible P-waves in the LFE stacks, most locations have poor depth control so we fix their depths to the plate interface. Of the remaining four events, highlighted by thick black in Fig. 3, we find depths ranging from 31 to 34 km using the velocity model of Williams et al. (2011). Alternatively, using the O0 model, we find that the depths of the four LFEs mentioned above increases by an average of 4 km.

The location and timing of events agree with the spatiotemporal migration of tremor and slip in this region. Both the geodetic slip inversion of Bartlow et al. (2011) and automated tremor locations of Wech and Creager (2008) indicate that slip in the 2009 event propagated from north to south and arrives in central Oregon in late August (25th). In our families, the arrival of the main slip front manifests as a sharp increase in the detection rate (many detections prior to the SSE are likely false), which first occurs in the northernmost families (Fig. 3B) on August 30th and propagates south at a rate of 5 km/day, consistent with observations of other SSEs in Cascadia (Boyarko and Brudzinski, 2010; Royer et al., 2015). Additionally, the geodetic and tremor data indicate that the 2009 SSE ceased just south of the densest station spacing around the latitude of Eugene consistent with our detection rates decreasing to pre-SSE levels.

4. Discussion

SSEs and associated NVT occur regularly in Oregon. While autocorrelation is routinely employed to identify repeating earthquakes, in central Oregon, that method systematically fails due to the low SNR of many stations, low station density, and the infrequent occurrence of isolated LFEs (i.e., LFEs tend to occur in rapid succession). We find that the cross-station approach of Savard and Bostock (2014) is more successful at identifying individual LFEs. These individual candidate LFE templates can then be used in an iterative network cross-correlation and stacking routine to identify additional repeats and refine the template (if enough repeats of that LFE are detected).

Both sets of locations reported in the Results section are generally consistent with LFEs in central Oregon locating at or near the plate interface as reported in similar studies of LFEs in the northern and southern parts of the Cascadia subduction zone (Bostock et al., 2012; Plourde et al., 2015; Royer and Bostock, 2014). While slightly shallower than the plate interface models of McCrory et al. (2004) and Audet et al. (2010), our preferred locations are those calculated using the local velocity model of Williams et al. (2011) because the depths of LFEs located using this model are closer to the depths of both interface models. LFE epicenters are consistent with tremor distributions that occur approximately 50 km inland from the shallow edge of the geodetically inferred transition zone (Boyarko and Brudzinski, 2010; Burgette et al., 2009). Magnetotelluric data analyzed by Wannamaker et al. (2014) indicate that central Cascadia has an expansive zone of low resistivity material, thought to represent subducting sediments, extending from ~10 to 40 km depth along the plate interface. Those authors suggest that dewatering and frictional properties of significant underthrust sediments can explain the large extent of the geodetic transition zone, generally low coupling, and the fact that LFEs in central Cascadia appear to occur farther up dip from the inferred onset of eclogitization Wannamaker et al. (2014).

A comparison between our templates and those beneath southern Vancouver Island and in northern California reveals that LFEs in central and southern Cascadia appear to have more complicated waveforms at similar epicentral distances and for a similar number of contributing detections. Bostock et al. (2012) reported that many of the templates
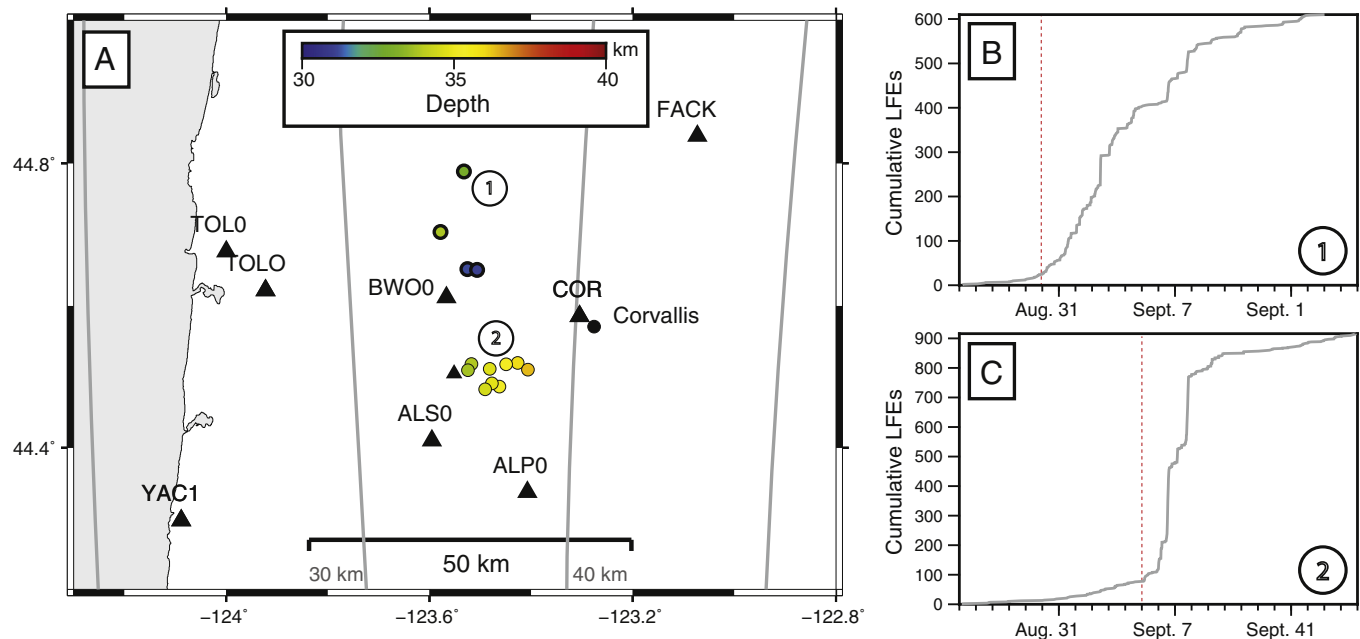

Fig. 3. (A) Epicenters of the 13 locatable LFE families color coded by depth. Depths for the northernmost four families (thick black outlines) were determined from HYPOINVERSE, while the depths of the remaining families were assigned to the plate interface. (B and C) The total number of LFEs detected vs. time for two families (1 and 2) whose locations are indicated in panel A. Vertical dashed red lines indicate approximate SSE arrival times evidenced by an increase in detection rate.
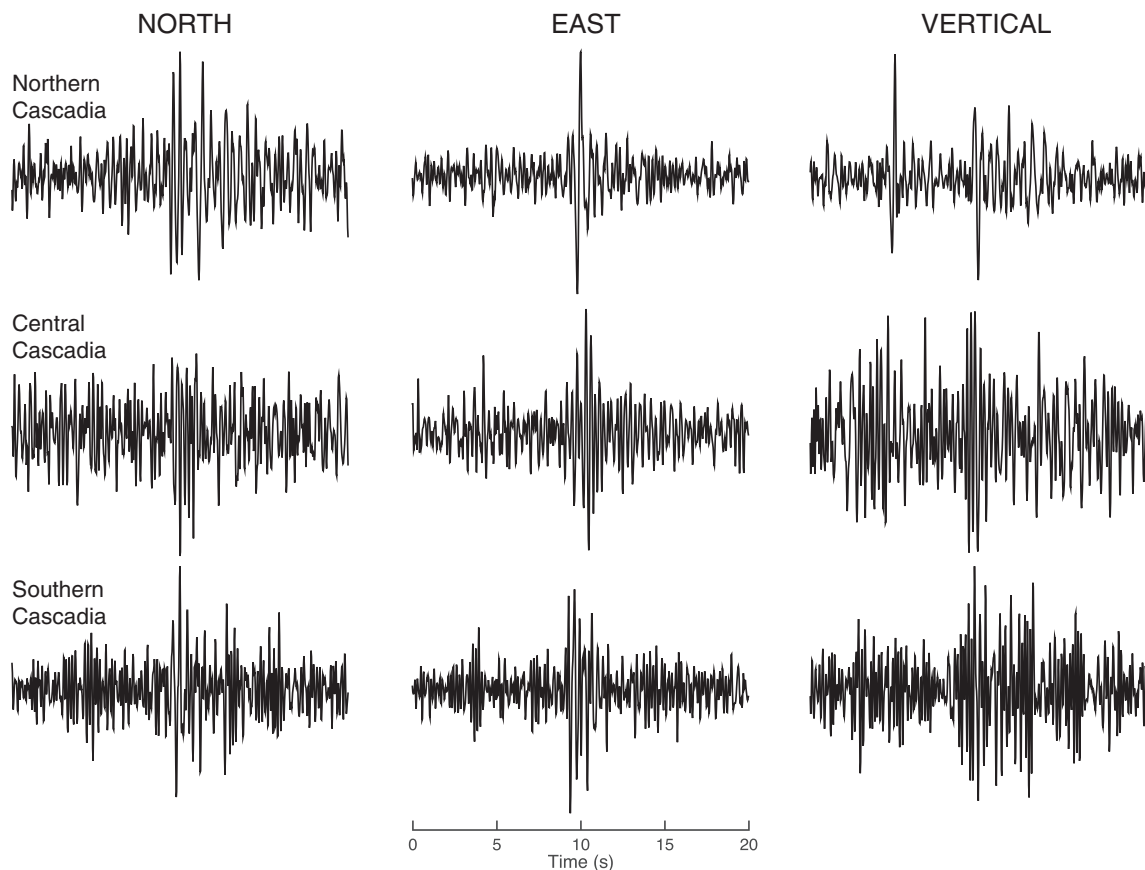
Fig. 4. Comparison of three component LFE templates from northern, central, and southern Cascadia from Royer and Bostock (2014), this study, and Plourde et al. (2015), respectively. All three templates are centered on the S wave arrival, have similar epicentral distances (30 km), and represent stacks of a similar number of contributing detections (300). Northern Cascadia data are from station KNLB, central Cascadia data are from ALS0, and southern Cascadia data are from ME29.

assembled in that study were simple waveforms with abrupt onset and visible P and S waves (top row in Fig. 4). In contrast, our templates and those in southern Cascadia (middle and bottom rows in Fig. 4) generally have more emergent arrivals, sustained coda, and P-waves that are only visible on a small fraction of families. While path effects and the LFE source may contribute in part to waveform complexity, the differences in waveform character, particularly the lack of P-waves, are most likely due to the small number of contributing stations in central and southern Cascadia. The stations we employed in the cross-station analysis have similar SNR to those used to detect LFEs in northern Cascadia; however, fewer stations result in detections that are less spatially precise than those in southern Vancouver Island. Stacking of waveforms that originate from a larger spatial footprint can obscure template features, resulting in templates that are not as clean as those in regions with better station coverage.

The differences in waveform character could also be due in part to false detections. Assuming, as a worst case scenario, that the detection rate prior to the arrival of the SSE in Oregon is representative of the false detection rate, relatively high-quality templates, such as the one shown in Fig. 2, have 2–3 false detections per day, while over 700 events over a 3-day period were used in template construction. In this particular case, false detections do not influence template quality in any significant way. False detections may influence waveform character in families that have higher false detection rates of 10 events/day and were assembled using a smaller number of detections; however, a comparison of the pre-SSE event rate and the total number of events used to assemble template waveforms of our 18 families suggest this effect is minimal. Additionally, the pre-SSE detection rate is likely an overestimate of the false detection rate, as in many cases stacking pre-SSE detections results in coherent templates albeit with lower SNR. Future work

will focus on refining LFE locations and studying more recent SSEs with better station coverage.

5. Conclusions

We identified 18 LFE families in central Cascadia using a combination of a cross-station method to identify potential templates and network cross-correlation to register additional detections. The majority of events locate to the west of Corvallis either at or slightly shallower than the plate interface model of McCrory et al. (2004). The time history of detections between families is consistent with the slip front in the 2009 SSE migrating from north to south at a velocity of 5 km/day. The templates we have identified are more complicated than those previously identified in northern Cascadia. Template quality may be affected by both false LFE detections and stacking detections over a larger hypocentral footprint.

References

Audet, P., Bostock, M.G., Boyarko, D.C., Brudzinski, M.R., Allen, R.M., 2010. Slab morphology in the Cascadia fore arc and its relation to episodic tremor and slip. J. Geophys. Res. Solid Earth (1978–2012) 115 (B4).

Bartlow, N.M., Miyazaki, S., Bradley, A.M., Segall, P., 2011. Space-time correlation of slip and tremor during the 2009 Cascadia slow slip event. Geophys. Res. Lett. 38. http://dx.doi.org/10.1029/2011GL048714.

Bostock, M.G., Royer, A.A., Hearn, E.H., Peacock, S.M., 2012. Low frequency earthquakes below southern Vancouver Island. Geochem. Geophys. Geosyst. 13, 11007. http://dx.doi.org/10.1029/2012GC004391.

Boyarko, D.C., Brudzinski, M.R., 2010. Spatial and temporal patterns of nonvolcanic tremor along the southern Cascadia subduction zone. J. Geophys. Res. Solid Earth 115. http://dx.doi.org/10.1029/2008JB006064.

Brown, J.R., Beroza, G.C., Ide, S., Ohta, K., Shelly, D.R., Schwartz, S.Y., Rabbel, W., Thorwart, M., Kao, H., 2009. Deep low-frequency earthquakes in tremor localize to the plate interface in multiple subduction zones. Geophys. Res. Lett. 36. http://dx.doi.org/10.1029/2009GL040027.

Burgette, R.J., Weldon, R.J., Schmidt, D.A., 2009. Interseismic uplift rates for western Oregon and along-strike variation in locking on the Cascadia subduction zone. J. Geophys. Res. Solid Earth (1978–2012) 114 (B1).

Chamberlain, C.J., Shelly, D.R., Townend, J., Stern, T.A., 2014. Low-frequency earthquakes reveal punctuated slow slip on the deep extent of the Alpine Fault, New Zealand. Geochem. Geophys. Geosyst. 15 (7), 2984–2999.

Frank, W., Shapiro, N., 2014. Automatic detection of low-frequency earthquakes (lfes) based on a beamformed network response. Geophys. J. Int. 197 (2), 1215–1223.

Frank, W.B., Shapiro, N.M., Kostoglodov, V., Husker, A.L., Campillo, M., Payero, J.S., Prieto, G.A., 2013. Low-frequency earthquakes in the Mexican sweet spot. Geophys. Res. Lett. 40 (11), 2661–2666.

Gerdom, M., Trehu, A., Flueh, E., Klaeschen, D., 2000. The continental margin off Oregon from seismic investigations. Tectonophysics 329 (1), 79–97.

Gibbons, S.J., Ringdal, F., 2006. The detection of low magnitude seismic events using array-based waveform correlation. Geophys. J. Int. 165 (1), 149–166.

Ide, S., Beroza, G.C., Shelly, D.R., Uchide, T., 2007. A scaling law for slow earthquakes. Nature 447, 76–79. http://dx.doi.org/10.1038/nature05780.

Klein, F.W., 2002. User's guide to HYPOINVERSE-2000: a Fortran program to solve for earthquake locations and magnitudes. US Geological Survey.

McCrory, P.A., Blair, J.L., Oppenheimer, D.H., Walter, S.R., 2004. Depth to the Juan de Fuca slab beneath the Cascadia subduction margin: a 3-D model for sorting earthquakes. US Department of the Interior, US Geological Survey.

Obara, K., 2002. Nonvolcanic deep tremor associated with subduction in southwest Japan. Science 296, 1679–1681. http://dx.doi.org/10.1126/science.1070378.

Plourde, A.P., Bostock, M.G., Audet, P., Thomas, A.M., 2015. Low-frequency earthquakes at the southern Cascadia margin. Geophys. Res. Lett. http://dx.doi.org/10.1002/2015GL064363 (2015GL064363).

Royer, A.A., Bostock, M.G., 2014. A comparative study of low frequency earthquake templates in northern Cascadia. Earth Planet. Sci. Lett. 402, 247–256.

Royer, A.A., Thomas, A.M., Bostock, M.G., 2015. Tidal modulation and triggering of low-frequency earthquakes in northern Cascadia. J. Geophys. Res. Solid Earth 120 (1), 384–405. http://dx.doi.org/10.1002/2014JB011430 (2014JB011430).

Rubin, A.M., Armbruster, J.G., 2013. Imaging slow slip fronts in Cascadia with high precision cross-station tremor locations. Geochem. Geophys. Geosyst. 14 (12), 5371–5392.

Savard, G., Bostock, M.G., 2014. Studies of low-frequency earthquakes in Northern Cascadia using a cross-station method. AGU Fall Meeting Abstracts 1, 4535.

Schimmel, M., Paulssen, H., 1997. Noise reduction and detection of weak, coherent signals through phase-weighted stacks. Geophys. J. Int. 130 (2), 497–505.

Shelly, D.R., Hardebeck, J.L., 2010. Precise tremor source locations and amplitude variations along the lower-crustal central San Andreas Fault. Geophys. Res. Lett. 37. http://dx.doi.org/10.1029/2010GL043672.

Shelly, D.R., Beroza, G.C., Ide, S., Nakamula, S., 2006. Low-frequency earthquakes in Shikoku, Japan, and their relationship to episodic tremor and slip. Nature 442, 188–191. http://dx.doi.org/10.1038/nature04931.

Shelly, D.R., Beroza, G.C., Ide, S., 2007. Non-volcanic tremor and low-frequency earthquake swarms. Nature 446, 305–307. http://dx.doi.org/10.1038/nature05666.

Tang, C.C., Peng, Z., Chao, K., Chen, C.H., Lin, C.H., 2010. Detecting low-frequency earthquakes within non-volcanic tremor in southern Taiwan triggered by the 2005 Mw8.6 Nias earthquake. Geophys. Res. Lett. 37 (16).

Thurber, C.H., Zeng, X., Thomas, A.M., Audet, P., 2014. Phase-weighted stacking applied to low-frequency earthquakes. Bull. Seismol. Soc. Am. 104 (5), 2567–2572. http://dx.doi.org/10.1785/0120140077.

Tréhu, A.M., Braunmiller, J., Nabelek, J.L., 2008. Probable low-angle thrust earthquakes on the Juan de Fuca–North America plate boundary. Geology 36 (2), 127–130.

Wannamaker, P.E., Evans, R.L., Bedrosian, P.A., Unsworth, M.J., Maris, V., McGary, R.S., 2014. Segmentation of plate coupling, fate of subduction fluids, and modes of arc magmatism in Cascadia, inferred from magnetotelluric resistivity. Geochem. Geophys. Geosyst. 15 (11), 4230–4253.

Wech, A.G., Creager, K.C., 2008. Automated detection and location of Cascadia tremor. Geophys. Res. Lett. 35 (20).

Wessel, P., Smith, W.H., Scharroo, R., Luis, J., Wobbe, F., 2013. Generic mapping tools: improved version released. Eos Trans. AGU 94 (45), 409–410.

Williams, M.C., Tréhu, A.M., Braunmiller, J., 2011. Seismicity at the Cascadia plate boundary beneath the Oregon continental shelf. Bull. Seismol. Soc. Am. 101 (3), 940–950.